Evaluation of band offset at amorphous-Si/$BaSi_2$ interfaces by hard x-ray photoelectron spectroscopy

Ryota Takabe,[1] Hiroki Takeuchi,[1] Weijie Du,[1] Keita Ito,[1,2,3] Kaoru Toko,[1] Shigenori Ueda,[4,5] Akio Kimura,[6] and Takashi Suemasu[1]
[1]*Institute of Applied Physics, University of Tsukuba, Tsukuba, Ibaraki 305-8573, Japan*
[2]*Japan Society for the Promotion of Science (JSPS), Chiyoda, Tokyo 102-0083, Japan*
[3]*Department of Electronic Engineering, Graduate School of Engineering, Tohoku University, Sendai 980-8579, Japan*
[4]*Synchrotron X-Ray Station at SPring-8, National Institute for Materials Science (NIMS), Sayo, Hyogo 679-5148, Japan*
[5]*Quantum Beam Unit, NIMS, Tsukuba, Ibaraki 305-0047, Japan*
[6]*Graduate School of Science, Hiroshima University, Higashi-Hiroshima 739-8526, Japan*

(Received 10 February 2016; accepted 12 April 2016; published online 27 April 2016)

The 730 nm-thick undoped $BaSi_2$ films capped with 5 nm-thick amorphous Si (a-Si) intended for solar cell applications were grown on Si(111) by molecular beam epitaxy. The valence band (VB) offset at the interface between the $BaSi_2$ and the a-Si was measured by hard x-ray photoelectron spectroscopy to understand the carrier transport properties by the determination of the band offset at this heterointerface. We performed the depth-analysis by varying the take-off angle of photoelectrons as 15°, 30°, and 90° with respect to the sample surface to obtain the VB spectra of the $BaSi_2$ and the a-Si separately. It was found that the barrier height of the a-Si for holes in the $BaSi_2$ is approximately −0.2 eV, whereas the barrier height for electrons is approximately 0.6 eV. This result means that the holes generated in the $BaSi_2$ layer under solar radiation could be selectively extracted through the a-Si/$BaSi_2$ interface, promoting the carrier separation in the $BaSi_2$ layer. We therefore conclude that the a-Si/$BaSi_2$ interface is beneficial for $BaSi_2$ solar cells. *Published by AIP Publishing.*
[http://dx.doi.org/10.1063/1.4947501]

I. INTRODUCTION

Thin-film solar cells, such as Cu(In, Ga)Se_2 (CIGS),[1–4] CdTe,[5–7] and perovskite solar cells,[8–10] have drawn intense research interest because of their high energy conversion efficiency and low cost. However, these materials contain critical raw materials. Materials consisting of earth-abundant and environmental-friendly elements are preferable when we think of the future deployment of terawatt-scale solar cells. Si thin-film solar cells have thus been studied extensively;[11–15] however, it is not easy to achieve high conversion efficiency as large as 20% because of its small absorption coefficient, α. Among such materials, we have been studying orthorhombic barium disilicide ($BaSi_2$). $BaSi_2$ is a semiconducting silicide, which consists of earth-abundant Ba and Si, and has a band gap (ca. 1.3 eV) appropriate for a single-junction solar cell.[16] Besides, α reaches $3 \times 10^4\,cm^{-1}$ at 1.5 eV.[16] This value is more than 40 times larger than that of crystalline Si, which is $7 \times 10^2\,cm^{-1}$ at 1.5 eV.[17] In addition, undoped $BaSi_2$, which shows n-type conductivity with an electron concentration of the order of $10^{16}\,cm^{-3}$,[18] exhibits a large minority-carrier diffusion length $L \approx 10\,\mu m$ (Ref. 19) and a large minority-carrier lifetime $\tau \approx 10\,\mu s$.[20,21] Owing to large L and large α, we can expect an energy conversion efficiency to be larger than 25% only in a 2 μm-thick $BaSi_2$ pn junction diode.[22] For these reasons, $BaSi_2$ is a candidate material for high efficiency thin-film solar cells. For device application, surface passivation is very important for materials like $BaSi_2$, which possess large α, because the short-wavelength light is absorbed in the region close to the surface. For example, α reaches $4 \times 10^5\,cm^{-1}$ at a wavelength of 500 nm for $BaSi_2$,[16] meaning that most of the photons at this wavelength are absorbed as they pass only 75 nm ($1/\alpha \times 3 = 75$ nm) through the $BaSi_2$ layer, and electrons and holes are generated. Therefore, defective surface deteriorates the solar cell performance. Microwave-detected photoconductivity decay (μ-PCD) measurements showed that τ reaches approximately 10 μs with excellent repeatability for undoped $BaSi_2$ by means of capping the $BaSi_2$ surface with the native oxide or a few nanometers thick amorphous Si (a-Si) layer.[23] For the native oxide/undoped-$BaSi_2$ interface, we found that the barrier height of the native oxide for the minority-carriers, holes, in the undoped $BaSi_2$ is 3.9 eV.[24] The transport of holes generated under solar radiation is therefore blocked at the interface, resulting in the limited conversion efficiency $\eta \approx 0.1\%$ in a solar cell using the native oxide/$BaSi_2$ interface.[25] The short-circuit current density J_{SC} was only $0.2\,mA/cm^2$. On the other hand, we achieved $\eta = 9.0\%$ very recently in a solar cell utilizing the a-Si/$BaSi_2$ interface.[26] J_{SC} reached $31.9\,mA/cm^2$. Thereby, understanding of the band lineup at this heterointerface is very important. In this study, we formed the a-Si/undoped-$BaSi_2$ structure by molecular beam epitaxy (MBE) to measure the valence-band offset (VBO) by hard x-ray photoelectron spectroscopy (HAXPES) and also calculated the conduction band offset (CBO) at the interface from the measured VBO to understand the transport of carriers across the interface.

HAXPES is a fairly powerful method to analyze the VB density of states (DOS) of buried layers because of the large analysis depth.[27–35] Conventional x-ray photoelectron

spectroscopy with the electron kinetic energy of 50–100 eV is quite surface sensitive due to the short electron inelastic mean free path (IMFP), λ, of <5 Å.[36] It is thus difficult to analyze the electronic states inside solids. On the other hand, much larger IMFP ($\lambda > 50$ Å) in HAXPES enables us to measure the VB spectra of buried layers non-destructively. Besides, a reduced photoionization cross-section is compensated by an extremely brilliant x-ray provided from an undulator light source installed in the third generation synchrotron radiation facilities, enabling us to perform HAXPES measurements with high-energy resolution.[37–39] There have been several reports utilizing this large probing depth to measure VB spectra of buried layers such as native-oxide/$BaSi_2$, CdS/Cu_2ZnSnS_4 (CZTS), AlO_x/Si heterostructures, and Bi_2Se_3 surface.[24,33–35] In Ref. 33, for example, Tajima *et al*. have reported that the VBO at the CdS/CZTS interface was 0.0 ± 0.1 eV. It was determined from the VB spectra of CdS and CZTS, by changing the probing depth, which was controlled by take-off-angle (TOA) of photoelectrons in HAXPES.

II. EXPERIMENTAL METHOD

We fabricated a-Si(5 nm)/undoped-$BaSi_2$ (730 nm) structures by means of an ion-pumped MBE system with the base pressure of better than 10^{-8} Pa, equipped with a standard Knudsen cell for Ba and an electron-beam gun for Si. The procedure of the sample preparation is as follows. We first deposited Ba on an n-Si(111) ($\rho \leq 0.01$ Ω cm) substrate at 500 °C by reactive deposition epitaxy to form a 5 nm-thick $BaSi_2$ template layer.[40] This template acts as seed crystals for overlayers. We next co-deposited Ba and Si on the template at 580 °C by MBE to form undoped $BaSi_2$.[41,42] The *a*-axis-oriented epitaxial growth of $BaSi_2$ was confirmed by the reflection high-energy electron diffraction and x-ray diffraction. In sample A, a 730 nm-thick undoped $BaSi_2$ epitaxial film was capped *in situ* with a 5 nm-thick a-Si layer at 180 °C, followed by air exposure for 26 h. For sample B, we exposed a 600 nm-thick undoped $BaSi_2$ epitaxial film to the air for 26 h without any capping layers, on which a sufficiently thick (ca. 8 nm) native oxide layer was formed.[24] Sample structures for samples A and B are summarized in Table I. Cross-sectional transmission electron microscopy (TEM) observation was performed with an acceleration voltage of 200 kV to examine the cross sections of samples A and B. Thin foils for TEM observation were prepared with an ion beam micro-sampling system. We performed HAXPES measurement at room temperature at the revolver undulator beamline BL15XU[39,43] of SPring-8 in Japan. The excitation photon energy was set at 5953 eV and the incident angle of the photon was set to ca. 2°–11° with respect to the sample surface. The analysis depth was changed by controlling TOA of photoelectrons. The overall energy resolution was set to 155 meV. The Fermi energy, E_F, was referred to the Fermi cut-off of an evaporated Au film.

TABLE I. Sample preparation: $BaSi_2$ layer thickness, air exposure duration, and surface capping and its layer thickness are specified.

Sample	$BaSi_2$ layer (nm)	Air exposure duration (h)	Capping (nm)
A	730	26	5(a-Si)
B[24]	600	26	0 (native oxide 8 nm)

III. RESULTS AND DISCUSSION

The bright-field cross-sectional TEM images of samples A and B are given in Figs. 1(a) and 1(b), respectively. As shown in Fig. 1(a), a 5 nm-thick a-Si layer is uniformly formed on the $BaSi_2$ surface as expected and the a-Si/$BaSi_2$ interface has a sharp interface. The fact that the a-Si layer thickness was almost the same as the deposited thickness monitored by a quartz crystal microbalance system is the indication of that the oxidation of the a-Si would terminate near the surface. In contrast, the oxidation of the $BaSi_2$ progressed in sample B, and an approximately 8 nm-thick native oxide layer was formed on the $BaSi_2$.[24]

The wide range HAXPES spectra of samples A and B[24] taken at TOA = 90° are shown in Figs. 2(a) and 2(b), respectively. As can be seen in these figures, the Si core-level peaks such as Si 2*s* and 2*p* for sample A were stronger than those for sample B, whereas the O 1*s* core-level peak for sample B was stronger than that for sample A. This means that we can suppress the oxidation of the $BaSi_2$ layer by *in situ* capping with the a-Si layer. Before discussing the VBO at the a-Si/$BaSi_2$ interface, we compare the core-level spectra in the Ba $3d_{5/2}$ and Si 2*s* regions measured with different TOAs in order to examine the band bending near the a-Si/$BaSi_2$ interface. The IMFP value, λ, for $BaSi_2$ was calculated to be approximately 10 nm at 6 keV using the Tanuma-Powell-Penn (TPP-2M) equation,[36] and the probing depth is estimated to be $3\lambda \times \sin(\text{TOA})$; that is, approximately 8, 15, and 30 nm for TOA = 15°, 30°, and 90°, respectively.

Figure 3(a) shows the Ba $3d_{5/2}$ core-level spectra of sample A taken at TOA = 15°, 30°, and 90°. Figure 3(b) is the normalized spectra of Fig. 3(a) using the peak located at −780.6 eV. In Fig. 3(b), we see only one peak located at −780.6 eV at TOA = 30° and 90°. We attribute this peak to the $BaSi_2$ layer. In contrast, by the peak-fitting analysis, the spectrum measured at TOA = 15° was well reproduced by adding another Gaussian curve located at −781.1 eV, probably due to slight oxidation of $BaSi_2$ as described below.

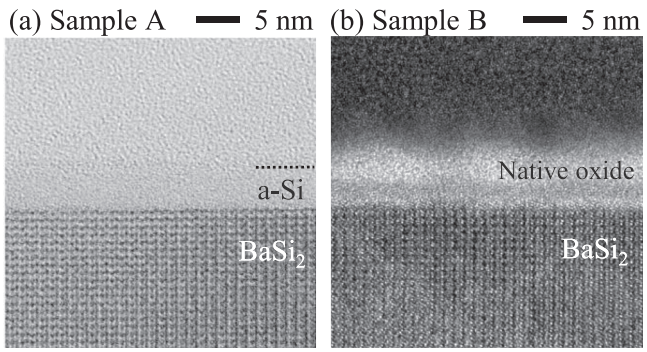

FIG. 1. Cross-sectional TEM images of (a) a-Si(5 nm)/$BaSi_2$(730 nm) (sample A) and (b) native oxide(ca. 8 nm)/$BaSi_2$(600 nm) (sample B). Reprinted with permission from J. Appl. Phys. **119**, 025306 (2016). Copyright 2016 AIP Publishing LLC.

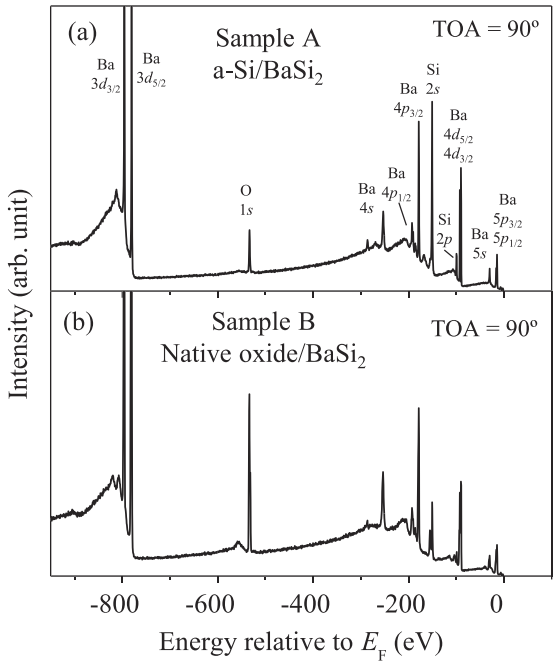

FIG. 2. Wide-range HAXPES spectra of (a) a-Si(5 nm)/$BaSi_2$(730 nm) (sample A) and (b) oxide(ca. 8 nm)/$BaSi_2$(600 nm) (sample B)[24] taken at TOA = 90°.

Figure 3(c) shows the Ba $3d_{5/2}$ core-level spectra of sample B, taken at TOA = 15°, 30°, and 90°. At TOA = 30° and 90°, each spectrum was well reproduced by two Gaussian curves located at −780.6 eV and −781.7 eV. At TOA = 15°, however, one Gaussian curve located at −781.7 eV was enough to reconstruct the measured spectrum. The peak located at −780.7 eV became stronger as TOA decreased. We therefore attribute this peak to the surface native oxide because the contribution of this peak appeared dominant in the surface-sensitive measurement (TOA = 15°). Hence, it is clear that the a-Si layer suppressed the oxidation of the $BaSi_2$ layer in sample A. Furthermore, the peak positions did not shift regardless of TOA (i.e., analysis depth) in Figs. 3(a) and 3(b), meaning that the band bending did not occur or it was negligibly small in the $BaSi_2$ near the a-Si/$BaSi_2$ interface.

Figure 4(a) shows the Si 2*s* core-level spectra for sample A, taken at TOA = 15°, 30°, and 90°. Figure 4(b) is the normalized spectra of Fig. 4(a) using the peak located around −151 eV. The ratio of the peak intensity around −155 eV to that around −151 eV increased as the TOA decreased, indicating that the peak around −155 eV was due to the surface oxides. Note that the peak position located around −151 eV was shifted by approximately 0.2 eV as TOA was decreased from 90° to 15°. As discussed before, the band bending did not occur in the $BaSi_2$ near the a-Si/$BaSi_2$ interface. Thereby, we attribute this peak shift to the band bending in the a-Si layer. As seen in Fig. 4(c), the peak intensities of oxides became stronger for sample B as TOA decreased; the peak located around −151 eV almost disappeared at TOA = 15°. Therefore, it is reasonable to consider that the a-Si suppressed the surface oxidation for sample A from the viewpoint of the Si 2*s* core-level spectra as well as the Ba $3d_{5/2}$ core-level spectra.

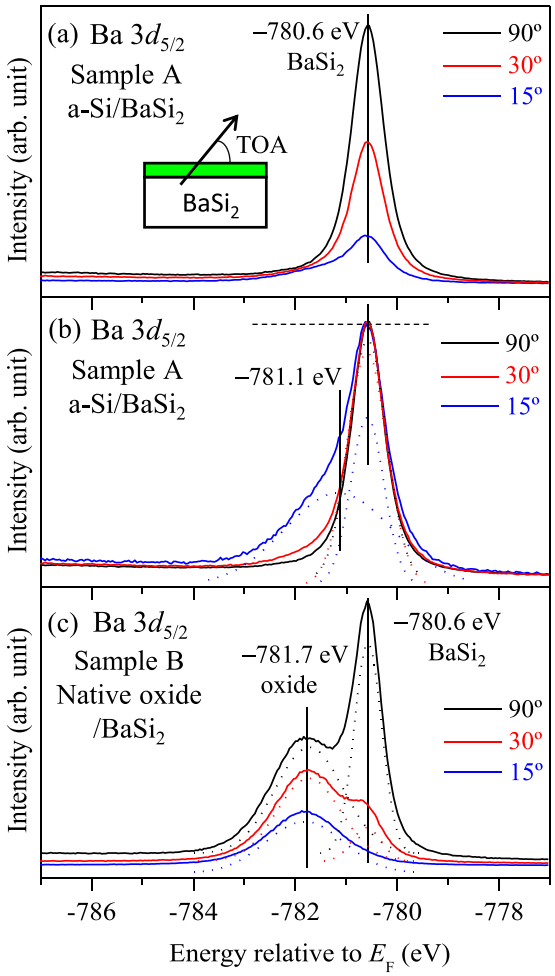

FIG. 3. Ba $3d_{5/2}$ core-level HAXPES spectra for (a) a-Si(5 nm)/$BaSi_2$(730 nm) (sample A), (b) normalized spectra of (a), and (c) oxide(ca. 8 nm)/$BaSi_2$(600 nm) (sample B)[24] taken at TOA = 15°, 30°, and 90°. The spectrum measured at TOA = 15° in (b) and the spectra measured at TOA = 30° and 90° in (c) can be fitted by the sum of two Gaussian curves (broken lines).

Figure 5(a) shows the calculated VB HAXPES spectrum of $BaSi_2$ obtained by the first-principles calculations, that is, the sum of the rescaled partial DOS of the Si 3*s*, Si 3*p*, and Ba 6*s* states by using their photo-ionization cross-sections at 6 keV. E_F is located in the middle of the band gap. Details of the calculation are given in our previous report.[44] The main VB feature of $BaSi_2$ extends from approximately −0.5 eV to −4 eV. We see the characteristic structures labeled A-C in Fig. 5(a). Structures A and C mainly consist of the Si 3*s* and Ba 6*s* states, and structure B is explained by the Si 3*s* state. Figures 5(b)–5(d) show the HAXPES spectra measured at different TOAs. The spectrum in Fig. 5(b) was measured under bulk-sensitive condition (TOA = 90°) and that in Fig. 5(d) under surface-sensitive condition (TOA = 15°). The VB HAXPES spectrum in Fig. 5(b) is quite similar to that calculated in Fig. 5(a). As one can see, the structures labeled *a*–*c* in Fig. 5(b) correspond to those labeled A–C in Fig. 5(a). At TOA = 30°, the intensity of the VB spectrum due to $BaSi_2$ decreased as seen in Fig. 5(c). When the TOA decreased further down to 15°, structure *c* almost disappeared as seen in Fig. 5(d). As shown in Figs. 5(a) and 5(b), structure

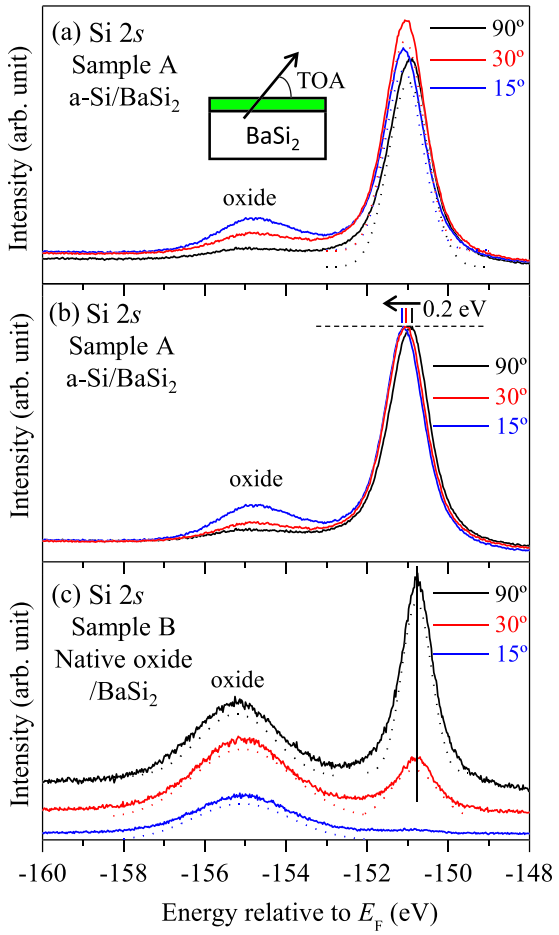

FIG. 4. Si 2*s* core-level HAXPES spectra for (a) a-Si(5 nm)/$BaSi_2$(730 nm) (sample A), (b) normalized spectra of (a), and (c) oxide(ca. 8 nm)/$BaSi_2$(600 nm) (sample B)[24] taken at TOA = 15°, 30°, and 90°. The spectra measured at TOA = 30° and 90° in (c) can be reconstructed by the sum of two Gaussian curves (broken lines).

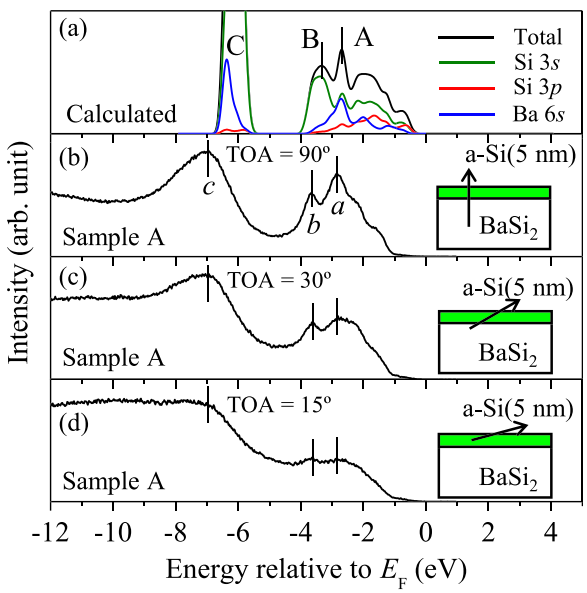

FIG. 5. (a) Calculated[43] and experimental HAXPES spectra of a-Si(5 nm)/$BaSi_2$(730 nm) (sample A) when the TOA is (b) 90°, (c) 30°, and (d) 15°. Schematics of sample structure and TOA denoted by arrows are also shown.

c originates from $BaSi_2$. Thereby, it is reasonable to consider that the VB HAXPES spectrum in Fig. 5(d) is not attributed to the $BaSi_2$ layer but to the a-Si layer.

Figures 6(a) and 6(b), respectively, show the HAXPES spectrum for sample A around −1.0 eV in Figs. 5(b) and 5(d), which are near the VB maximum (VBM) of $BaSi_2$, E_V^{BaSi2}, and near the VBM of a-Si, E_V^{a-Si}. We evaluated E_V^{BaSi2} and E_V^{a-Si} to be −1.06 eV and −0.96 eV, respectively, with respect to E_F by means of the linear extrapolation to the baseline. The obtained value of E_V^{a-Si} is consistent with the photoelectron spectroscopic investigations performed on very thin a-Si layers on a-Si substrate.[45] Figure 7 depicts the band lineup at the a-Si/undoped-$BaSi_2$ interface on the basis of these results. Assuming that the measured value of $E_F - E_V^{a-Si}$ (0.96 eV) is the mean value averaged over the 5 nm-thick a-Si, and the optical band gap of a-Si, E_g^{a-Si}, is approximately 1.7 eV,[46] VBO is calculated to be approximately 0.2 eV ($\approx 1.06 - 0.96 + \frac{0.2}{2}$), and CBO is derived to be approximately 0.6 eV ($\approx 0.2 + 1.7 - 1.3$). These results lead to the conclusion that the barrier height of the a-Si for holes in the undoped $BaSi_2$ is approximately −0.2 eV. This value is much smaller than 3.9 eV obtained for the native oxide/undoped $BaSi_2$ interface.[24] Therefore, the transport of photogenerated holes in the $BaSi_2$ under solar radiation is not hindered by the a-Si capping layer. On the other hand, the electrons in the $BaSi_2$ are blocked by the CBO at the interface. This means that the electrons and holes generated in the n-$BaSi_2$ layer under solar radiation are separated by the VBO and CBO at the interface, which is beneficial for solar cell applications. Hence, we conclude that the a-Si capping

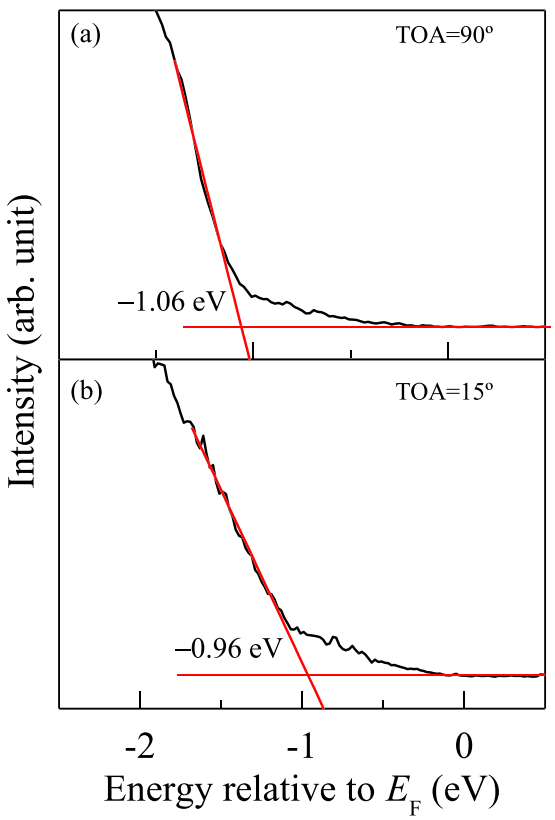

FIG. 6. Enlarged spectra for sample A around −1 eV taken at TOA = (a) 90° and (b) 15° around the VBM of $BaSi_2$ and a-Si, respectively.

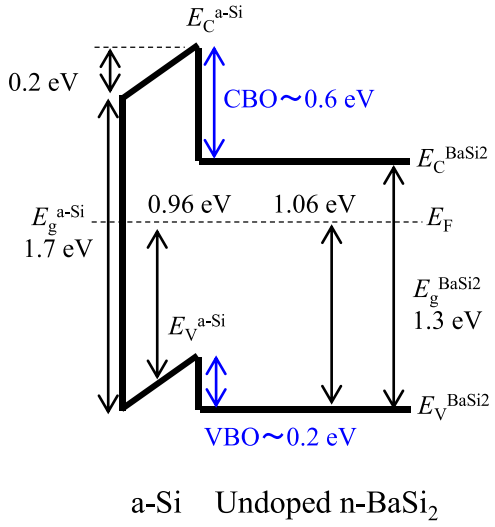

FIG. 7. Band lineup of the a-Si and $BaSi_2$ layers determined by the HAXPES measurements.

layer is effective not only on the improvement of the minority-carrier lifetime of $BaSi_2$ but also on the carrier separation in the $BaSi_2$ across the a-Si/$BaSi_2$ interface.

IV. SUMMARY

We formed 730 nm-thick undoped $BaSi_2$ epitaxial films capped *in situ* with the 5 nm-thick a-Si layer on Si(111) by MBE, and measured the electronic states of the buried $BaSi_2$ layer by HAXPES. We performed the depth-analysis by varying TOA of 15°, 30°, and 90°, and obtained the VB spectra of the $BaSi_2$ and the a-Si separately. The Ba $3d_{5/2}$ core-level peak did not shift regardless of TOA. This result revealed that the band bending did not occur in the $BaSi_2$ near the a-Si/$BaSi_2$ interface. In contrast, the band bending of the a-Si layer was approximately 0.2 eV from the shift of the Si 2*s* core-level peak. The VBM was located at −1.06 eV with respect to E_F for $BaSi_2$ and −0.96 eV for a-Si. We calculated the barrier height of the a-Si for holes in the $BaSi_2$ to be approximately −0.2 eV and that for electrons to be approximately 0.6 eV. We therefore conclude that the a-Si capping layer acts as a good electrical contact for hole transport in the a-Si/undoped-$BaSi_2$ structure as well as the surface passivation layer.

ACKNOWLEDGMENTS

The HAXPES measurements were conducted at Synchrotron X-ray station of BL15XU, at SPring-8, and were supported by NIMS microstructural characterization platform as a program of "Nanotechnology platform" (Proposal Nos. 2014A4902, 2015A4907, and 2015B4906) of the Ministry of Education, Culture, Sports, Science and Technology (MEXT), Japan. S.U. and A.K. are grateful to HiSOR, Hiroshima University, and JAEA at SPring-8 for the development of HAXPES at BL15XU. The authors thank Dr. N. Yoshizawa and Mr. N. Saito in AIST, Japan, for their help in TEM observations. This work was financially supported by the Japan Science and Technology Agency (JST/CREST) and by a Grant-in-Aid for Scientific Research (A) (No. 15H02237) from the JSPS. R.T. was financially supported by a Grant-in-aid for JSPS Fellows (No. 15J02139).

[1]P. Jackson, D. Hariskos, R. Wuerz, O. Kiowski, A. Bauer, T. M. Friedlmeier, and M. Powalla, Phys. Status Solidi RRL **9**, 28 (2015).
[2]I. Repins, M. A. Contreras, B. Egaas, C. DeHart, J. Scharf, C. L. Perkins, B. To, and R. Noufi, Prog. Photovoltaics **16**, 235 (2008).
[3]S. Merdes, F. Ziem, T. Lavrenko, T. Walter, I. Lauermann, M. Klingsporn, S. Schmidt, F. Hergert, and R. Schlatmann, Prog. Photovoltaics **23**, 1493 (2015).
[4]A. Chirila, P. Reinhard, F. Pianezzi, P. Bloesch, A. R. Uhl, C. Fella, L. Kranz, D. Keller, C. Gretener, H. Hagendorfer, D. Jaeger, R. Erni, S. Nishiwaki, S. Buecheler, and A. Tiwari, Nat. Mater. **12**, 1107 (2013).
[5]H. A. Mohamed, Thin Solid Films **589**, 72 (2015).
[6]X. Wu, Sol. Energy **77**, 803 (2004).
[7]C. Li, Y. Wu, J. Poplawsky, T. J. Pennycook, N. Paudel, W. Yin, S. J. Haigh, M. P. Oxley, A. R. Lupini, M. Al-Jassim, S. J. Pennycook, and Y. Yan, Phys. Rev. Lett. **112**, 156103 (2014).
[8]H. S. Kim, C. R. Lee, J. H. Im, K. B. Lee, T. Moehl, A. Marchioro, S. J. Moon, R. Humphry-Baker, J. H. Yum, J. E. Moser, M. Grätzel, and N. G. Park, Sci. Rep. **2**, 591 (2012).
[9]J. Burschka, N. Pellet, S.-J. Moon, R. Humphry-Baker, P. Gao, M. K. Nazeeruddin, and M. Grätzel, Nature **499**, 316 (2013).
[10]Y. Yamada, T. Nakamura, M. Endo, A. Wakamiya, and Y. Kanemitsu, J. Am. Chem. Soc. **136**, 11610 (2014).
[11]J. Müller, B. Rech, J. Springer, and M. Vanecek, Sol. Energy **77**, 917 (2004).
[12]A. V. Shah, H. Schade, M. Vanecek, J. Meier, E. Vallat-Sauvain, N. Wyrsch, U. Kroll, C. Droz, and J. Bailat, Prog. Photovoltaics **12**, 113 (2004).
[13]M. Konagai, Jpn. J. Appl. Phys., Part 1 **50**, 030001 (2011).
[14]B. Liu, L. Bai, Z. Chen, X. Zhang, D. Zhang, J. Ni, Q. Huang, C. Wei, J. Sun, X. Chen, H. Ren, G. Hou, G. Wang, and Y. Zhao, Prog. Photovoltaics: Res. Appl. **23**, 1313 (2015).
[15]H. Sai, T. Matsui, K. Saito, M. Kondo, and I. Yoshida, Prog. Photovoltaics: Res. Appl. **23**, 1572 (2015).
[16]K. Toh, T. Saito, and T. Suemasu, Jpn. J. Appl. Phys., Part 1 **50**, 068001 (2011).
[17]M. A. Green and M. J. Keevers, Prog. Photovoltaics: Res. Appl. **3**, 189 (1995).
[18]W. Du, M. Baba, K. Toko, K. O. Hara, K. Watanabe, T. Sekiguchi, N. Usami, and T. Suemasu, J. Appl. Phys. **115**, 223701 (2014).
[19]M. Baba, K. Toh, K. Toko, N. Saito, N. Yoshizawa, K. Jiptner, T. Sakiguchi, K. O. Hara, N. Usami, and T. Suemasu, J. Cryst. Growth **348**, 75 (2012).
[20]K. O. Hara, N. Usami, K. Toh, M. Baba, K. Toko, and T. Suemasu, J. Appl. Phys. **112**, 083108 (2012).
[21]K. O. Hara, N. Usami, K. Nakamura, R. Takabe, M. Baba, K. Toko, and T. Suemasu, Appl. Phys. Express **6**, 112302 (2013).
[22]T. Suemasu, Jpn. J. Appl. Phys., Part 1 **54**, 07JA01 (2015).
[23]R. Takabe, K. O. Hara, M. Baba, W. Du, N. Shimada, K. Toko, N. Usami, and T. Suemasu, J. Appl. Phys. **115**, 193510 (2014).
[24]R. Takabe, W. Du, K. Ito, H. Takeuchi, K. Toko, S. Ueda, A. Kimura, and T. Suemasu, J. Appl. Phys. **119**, 025306 (2016).
[25]W. Du, R. Takabe, M. Baba, H. Takeuchi, K. O. Hara, K. Toko, N. Usami, and T. Suemasu, Appl. Phys. Lett. **106**, 122104 (2015).
[26]D. Tsukahara, S. Yachi, H. Takeuchi, R. Takabe, W. Du, M. Baba, Y. Li, K. Toko, N. Usami, and T. Suemasu, Appl. Phys. Lett. **108**, 152101 (2016).
[27]L. Kövér, J. Electron Spectrosc. Relat. Phenom. **178–179**, 241 (2010).
[28]J. Rubio-Zuazo and G. R. Castro, Surf. Interface Anal. **40**, 1438 (2008).
[29]G. Panaccione and K. Kobayashi, Surf. Sci. **606**, 125 (2012).
[30]M. C. Mugumaoderha, R. Sporken, J. Ghijsen, and J. A. Dumont, J. Phys. Chem. C **115**, 20603 (2011).
[31]T. Nagata, S. Oh, Y. Yamashita, H. Yoshikawa, N. Ikeno, K. Kobayashi, T. Chikyow, and Y. Wakayama, Appl. Phys. Lett. **102**, 043302 (2013).
[32]D. Gerlach, R. G. Wilks, D. Wippler, M. Wimmer, M. Lozac'h, R. Félix, A. Mück, M. Meier, S. Ueda, H. Yoshikawa, M. Gorgoi, K. Lips, B. Rech, M. Sumiya, J. Hüpkes, K. Kobayashi, and M. Bär, Appl. Phys. Lett. **103**, 023903 (2013).
[33]S. Tajima, K. Kataoka, N. Takahashi, Y. Kimoto, T. Fukano, M. Hasegawa, and H. Hazama, Appl. Phys. Lett. **103**, 243906 (2013).

[34]N. Ikeno, Y. Yamashita, H. Oji, S. Miki, K. Arafune, H. Yoshida, S. Satoh, I. Hirosawa, T. Chikyow, and A. Ogura, Jpn. J. Appl. Phys., Part 1 **54**, 08KD19 (2015).
[35]C. E. ViolBarbosa, C. Shekhar, B. Yan, S. Ouardi, E. Ikenaga, G. H. Fecher, and C. Felser, Phys. Rev. B **88**, 195128 (2013).
[36]S. Tanuma, C. J. Powell, and D. R. Penn, Surf. Interface Anal. **43**, 689 (2011).
[37]M. B. Trzhaskovskaya, V. I. Nefedov, and V. G. Yarzhemsky, At. Data Nucl. Data Tables **77**, 97 (2001).
[38]M. B. Trzhaskovskaya, V. I. Nefedov, and V. G. Yarzhemsky, At. Data Nucl. Data Tables **82**, 257 (2002).
[39]S. Ueda, Y. Katsuya, M. Tanaka, H. Yoshikawa, Y. Yamashita, S. Ishimaru, Y. Matsushita, and K. Kobayashi, AIP Conf. Proc. **1234**, 403 (2010).
[40]Y. Inomata, T. Nakamura, T. Suemasu, and F. Hasegawa, Jpn. J. Appl. Phys., Part 1 **43**, 4155 (2004).
[41]Y. Inomata, T. Nakamura, T. Suemasu, and F. Hasegawa, Jpn. J. Appl. Phys., Part 2 **43**, L478 (2004).
[42]R. Takabe, K. Nakamura, M. Baba, W. Du, M. A. Khan, K. Toko, M. Sasase, K. O. Hara, N. Usami, and T. Suemasu, Jpn. J. Appl. Phys., Part 1 **53**, 04ER04 (2014).
[43]S. Ueda, J. Electron Spectrosc. Relat. Phenom. **190**, 235 (2013).
[44]M. Baba, K. Ito, W. Du, T. Sanai, K. Okamoto, K. Toko, S. Ueda, Y. Imai, A. Kimura, and T. Sueamsu, J. Appl. Phys. **114**, 123702 (2013).
[45]M. Schmidt, A. Schoepke, O. Milch, Th. Lussky, and W. Fuhs, MRS Proc. **762**, A19.11 (2003).
[46]K. Fukutani, M. Kanbe, W. Futako, B. Kaplan, T. Kamiya, and C. M. Fortmann, J. Non-Cryst. Solids **227–230**, 63 (1998).